The Sunyaev-Zeldovich effect

Etienne Pointecouteau[1,2]

[1] CNRS; IRAP; 9 Av. colonel Roche, BP 44346, F-31028 Toulouse cedex 4, France
[2] Université de Toulouse; UPS-OMP; IRAP; Toulouse, France
   e-mail: `etienne.pointecouteau@irap.omp.eu`

Abstract. The Sunyaev-Zeldovich (SZ) effect provides an alternative to X-rays to characterise the hot gas within groups and clusters. The past years have seen a drastic increase of number of SZ measurements. Experiments such as the *Planck* satellite, the South Pole Telescope, the Atacama Cosmology Telescope, the CARMA observatory, the Mustang/GBT instrument now allow precise SZ measurements over a wide range of spatial resolutions and frequency bands. These SZ observations are covering huge volumes and providing detailed measurements of the intra-cluster gas, now able to compete with X-ray data. But even more important, combined SZ and X-ray analysis bear a tremendous scientific potential for clusters studies in the framework of structure formation and evolution, as well as cosmology.

Key words. Cosmology: observations – Galaxies: clusters: intracluster medium – Submillimeter: diffuse background

1. Introduction

The inverse Compton scattering for thermalised electrons under a blackbody radiation field was formalised in the case of the hot gas content in galaxy clusters by Sunyaev & Zeldovich (1972). These authors predicted an ensuing spectral distortion of the CMB spectrum in the direction of clusters, the now so called Sunyaev-Zeldovich (SZ) effect.

The differential monochromatic brightness for the SZ effect can be expressed under the following generic form:

$$\frac{\Delta I_\nu}{I_\nu} = y \cdot \zeta(\nu, T_e) \qquad (1)$$

where ζ is a function expressing the spectral dependance of the SZ effect. This function

---

Send offprint requests to: E. Pointecouteau

mildly depends on the gas temperature through the weakly relativistic high end of the electron velocity distribution (see, e.g., Pointecouteau et al. 1998; Sazonov & Sunyaev 1998). If these relativistic effect, of order kT_e/mc^2, are neglected, the treatment of the inverse Compton scattering for thermalised electrons under a blackbody radiation field is obtained by the Kompaneets (1957) equation. With respect to the exact case, this approximation produces less scattering towards the high energy end of the spectrum thus respectively slightly increasing the absolute depth of the SZ increment at sub-millimetre wavelengths and of the decrement at millimetre wavelengths. Conversely the sub-millimetre tail of the SZ spectrum is reduced. Both exact and analytical expression are illustrated on Fig 1.

The dimensionless Comptonisation parameter y reads as the product of the average en-
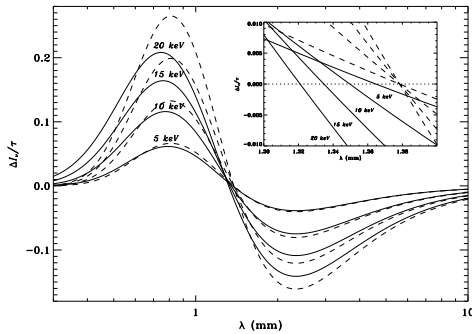
Fig. 1. Spectral dependance of the SZ effect. Figure reprinted from Pointecouteau et al. (1998). The solid line stands for the exact case (Eq. 1), where the dashed line show the analytical approximation for various intra-cluster gas temperatures.

ergy transferred per diffusion by the average number of diffusion:

$$y = \frac{\sigma_T}{m_e c^2} \int P(l)dl, \qquad (2)$$

where σ_T is the Thomson cross-section, m_e the mass of the electron and c the speed of light. P is the pressure produced by the plasma of thermal electrons along the line of sight.

If the SZ brightness, which is proportional to y, is independent of redshift, the SZ flux is proportional to the integrated Comptonisation parameter and thus depends on the source distance.

In the following, we leave aside the kinetic SZ effect, a doppler effect, resulting from the cluster peculiar motion within the comoving reference frame of the Hubble flow.

2. New clusters detection and synergy with X-ray

In the past years the SZ measurements have moved from the first spatially resolved observations of individual objects ((Pointecouteau et al. 2001; Komatsu et al. 2001, e.g.,)), to the first discoveries of new objects (Staniszewski et al. 2009), to large-scale survey projects for cosmology such as the *Atacama Cosmology Telescope* (Kosowsky 2003, *ACT)*, the *South Pole Telescope* (Carlstrom et al. 2011, *SPT)*

and the *Planck* satellite (Planck Collaboration I 2011). Pointed single dish and interferometric instruments such as SZA/CARMA (Muchovej et al. 2007), APEX-SZ (Dobbs et al. 2006), Mustang/GBT (Dicker et al. 2008), AMI (Zwart et al. 2008) or AMIBA (Ho et al. 2004) have further allowed detailed observations of specific clusters at different frequencies, resolutions and sensitivities.

With their large area survey capabilities, SPT, ACT and *Planck* are shading new light on the population of galaxy clusters. They have allowed the detection of tenths of new clusters previously unknown either in the optical or in the X-rays. The Early SZ sample encompassed 189 objects detected with high significance in the first *Planck* all-sky survey in nine frequency bands, providing for many clusters the first SZ measurement and also including new detected clusters (Planck Collaboration VIII 2011). The SPT collaboration has added 224 clusters detected over 720 square degrees at 150 and 95 GHz including about half new detected clusters (Reichardt et al. 2013). More recently a sample of 68 galaxy clusters, among which 19 new discoveries, were released by the ACT collaboration from their 148 GHz survey of 504 square degrees (Hasselfield et al. 2013).

These SZ clusters detections required systematically further multi-wavelengths follow-up in order (i) to confirm them as clusters, (ii) to estimate their redshift, (iii) to provide a characterisation of their global physical properties. The redshift estimations is provided either in the optical by photometric of spectroscopic redshift estimations (e.g. Bleem et al. 2012; Song et al. 2012) or from X-ray spectroscopy via the measurement of the Fe K line (e.g. Planck Collaboration XI 2011).

For new detected clusters, there is a real and powerful synergy between SZ and X-ray observation, as the X-rays provide a straightforward way to confirm candidates as clusters, as above the Galactic Plane, the detection of extended X–ray emission is an unambiguous signature of a cluster. This is illustrated for instance by the intense *XMM-Newton* validation follow-up programme run by the *Planck* collaboration with the *XMM-Newton* satellite: 51 observations of *Planck* cluster candidates have

led to 43 confirmation of new SZ sources. They have confirmed 51 *bona fide* new clusters, including four double systems and two triple systems (Planck Collaboration XI 2011; Planck Collaboration IV 2012). The SPT collaboration has made an extensive use of *Chandra* and *XMM-Newton* observations to characterise the physical properties of their detected clusters (Andersson et al. 2011).

Despite their more modest spatial coverage, SPT and ACT benefit a better spatial resolution, allowing them to hunt for more low mass and more distant clusters (e.g., Semler et al. 2012; Menanteau et al. 2012), therefore nicely complementing *Planck*'s findings of nearby clusters with low X-ray luminosities and disturbed morphologies.

3. Cosmology with the Sunyaev-Zeldovich effect

The total SZ signal is closely related to the cluster mass (e.g., da Silva et al. 2004), and its surface brightness insensitive to distance. Therefore, SZ surveys can potentially be used to built unbiased close to mass selected cluster samples up to high redshifts. Last structure to form in a hierarchical scenario of structure formation, clusters of galaxies are de facto extremely sensitive to the matter and energy content of the Universe. Cluster cosmology thus provides powerful and complementary constraints to CMB and other cosmological probes as shown by the recent results from SPT (Benson et al. 2011) and ACT (Sievers et al. 2013). The main caveats being that cluster cosmology is prone to systematics biases and errors linked to sample representativity and completeness, or to mass proxy calibration used to link the halo mass function (e.g., Pacaud et al. 2007).

Beyond cluster counts and the cluster mass function, the analysis of the SZ power spectrum (and/or bi- and tri-spectrum) also bring added information on cosmology and on our understanding of structure formation as shown by the recent measurement at low l mode (i.e., high angular resolution) of the CMB power-spectrum by SPT (Keisler et al. 2011) and ACT (Dunkley et al. 2011). These studies have em-

phasised the difficulty to disentangle the SZ contribution from the CIB and radio sources contribution to the power spectrum (i.e., with respect to the dumping CMB spectrum).

Constraints on cosmology from clusters are best optimised when combining the SZ signal with X-rays as done in the aforementioned work. We refer to the review by H. Böhringer (this proceedings) for further insights on cosmology with clusters.

4. Large scale structures

The scaling and structural properties expected in a hierarchical scenario of structure formation bear not only the imprint of the DM and DE, but also the complex physical processes at play throughout their formation and evolution (see e.g., Voit 2005, for a review). Recent X-ray observations based primarily on representative samples have returned a consistent picture of the scaling and structural properties of halos, from high mass clusters down to the low mass group regime (see, e.g., Vikhlinin et al. 2006; Croston et al. 2008; Pratt et al. 2009; Arnaud et al. 2010; Sun 2012).

From the SZ side, building on early works and measurements (Benson et al. 2004; Bonamente et al. 2008; Liao et al. 2010), approaches to constrain SZ/X-ray scaling relations (e.g., $Y_{500}-M_{500}$, $Y_{500}-L_{X,500}$) from small or medium size samples, spawning the nearby to the more distant Universe, have underlined the consistency between the X-ray and SZ view of the ICM within R_{500} (Andersson et al. 2011; Planck Collaboration IX 2011; Sifon et al. 2013). These results are also in agreement with complementary statistical analysis carried out over large sample of clusters on all-sky data from WMAP (Melin et al. 2011) and *Planck* (Planck Collaboration X 2011). Fig. 2 provides one illustration of this very coherent picture of our views for the hot thermal intra-clusters gas.
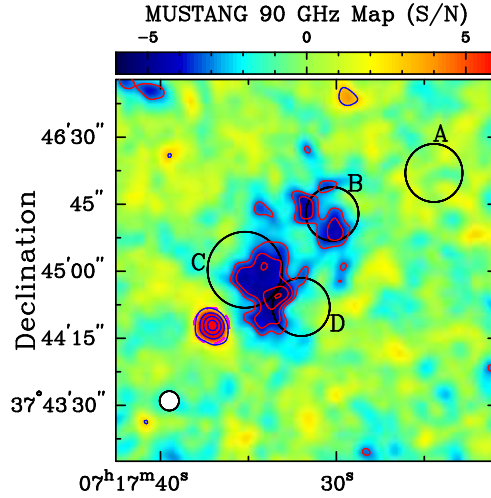
SZ and X-ray scaling relations have relied on X-ray observations that assume hydrostatic equilibrium for halos. As shown by various numerical simulations, this hypothesis likely results in a cluster mass systematically underestimated by about 10–15 percent due to the neglect of pressure support from bulk gas mo-
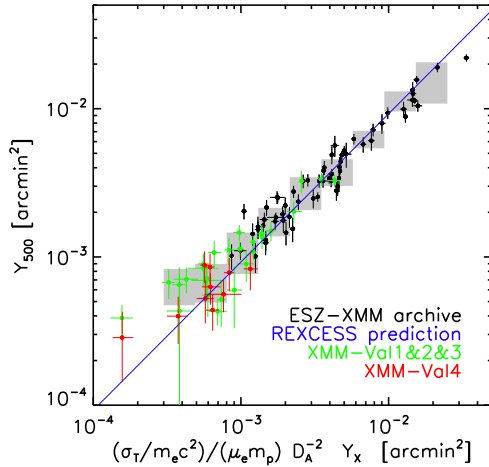
Fig. 2. The $Y_{500} - Y_X$ scaling relations derived from the *Planck* and *XMM-Newton* measurements. Figure reprinted from Planck Collaboration IV (2012).

Fig. 3. 90 GHz MUSTANG/GBT map of MACS J0717.5+3745 (13 arcsec resolution). Reprinted from Fig. 2 in Mroczkowski et al. (2012). See this publication for details.

tions in the HE mass equation (e.g., Nagai et al. 2007; Meneghetti et al. 2010). It is thus useful to call upon another mass proxy independent from both SZ and X-rays to investigate the impact of this "hydrostatic mass bias".

Weak lensing data provide a potential powerful way to estimate the cluster total mass, independent from the cluster baryons direct observations. Works by Marrone et al. (2012); Planck Collaboration III (2012) have shown an overall good agreement, between the SZ and lensing properties confronting SZA/CARMA and *Planck* SZ measurements respectively to weak lensing (WL) measurements (Subaru Telescope observations, Okabe et al. 2010). Though when adding a further comparison with X-ray results, Planck Collaboration III (2012) emphasised the differences between the X-ray and lensing mass proxies, that translate into a ∼ 20% normalisation offset on the SZ scaling relation. Focusing mainly in this proceedings on the SZ and X-ray measurements, we will not discuss here a third mass proxy, i.e., the optical richness, though it also bear several intrinsic biases and requires a very careful treatment. We refer to relevant works on the combination of SZ, X-rays and optical proxies (e.g., Planck Collaboration XXVI

2011; Draper et al. 2012; Sehgal et al. 2013; Angulo et al. 2012).

Inconsistency between the SZ, X-ray and optical data may arise from the combination of different effects and systematic biases, which as detailed by Angulo et al. (2012) can be twofold: (i) survey biases, and (ii) observable biases. The first type include discrepancies between samples selection (volume effect, Malmquist biases) ; or to foreground and background contamination. The second type is due to residual uncertainties on the instruments absolute calibration; or to projection, miscentering and orientation effects generating biases on the observables estimation; or the complex physics at play in clusters that render the extraction of observables more complicated (e.g., hydrostatic bias). All these effects affect in different ways X-ray, SZ and optical observations, and thus the slope, normalisation and intrinsic scatter of the different scaling relations.

5. Physics of the intracluster medium

Being a tracer of the thermal pressure, thus of the intra-cluster gas density and temperature,

the SZ signal has shown extremely efficient to probe the intra-cluster gas physics.

For instance, with the MUSTANG camera operated on the GBT telescope, Mroczkowski et al. (2012) have observed MACS J0717.5+3745, a complex-merger system comprising four distinct, optically detected sub-clusters, with a high spatial resolution (i.e., 13 arcsec at 90 GHz – see Fig. 3). Combined with Bolocam observation at 148 and 240 GHz, these observations allowed them a 2D comparison with the *Chandra* data. The unprecedented resolution for SZ observations together with Chandra sub-arcsec has confirmed previous indications from Chandra of a pressure enhancement due to shock-heated, ∼ 20 keV gas which is located next to an extended radio emission tracing non-thermal emission).

At very different spatial resolution scales, the *Planck* collaboration has also obtained stunning result in their analysis of the 2D distribution of the SZ signal in the direction of the Coma cluster. Thanks to its great sensitivity and frequency coverage, the *Planck* satellite was able to detect SZ emission out to $R \simeq 3 R_{500}$. Moreover, the *Planck* image shows a y profiles steepening locally about half a degree from the cluster centre to the West and to the South-East directions, underlying pressure jumps. These features are consistent with the presence of shock fronts at these radii. The western feature was indeed previously noticed in the ROSAT PSPC mosaic as well as in the radio. The *Planck* data finally revealed a strong linear correlation between the SZ and radio-synchrotron signal on a Mpc scale, implying either that the energy density of cosmic-ray electrons is relatively constant throughout the cluster, or that the magnetic fields fall off much more slowly with radius than previously thought.

These 2D studies are complemented by 1D radial analysis now reaching far our in the clusters outskirts. Indeed regions beyond R_{500} are hardly reachable by X-rays, but at the expense of huge amount of telescope time (Simionescu et al. 2011). Whereas SZ observations are really powerful here as shown by the recent study by the *Planck* Collaboration over a sample of 62 massive clusters. This statistical analysis has provided for the first time observational constraint on the gas thermal state and distribution out to $3 R_{500}$, where the density contrast is about 50–100 (Planck Collaboration V 2012). These results have been confirmed over a more modest radial range, i.e. ∼ $2 R_{500}$, by a later study of the Bolocam team from a sample of 45 clusters (Sayers et al. 2013). These SZ measurements allowed in both cases and in conjunction to X-ray data from *XMM-Newton* and *Chandra*, to reconstruct the average thermal pressure profiles in halos. These new results are already in fairly good agreement with theoretical predictions within the expected dispersion, and they also provide means to better understand together with theoretical approaches (e.g., Kravtsov & Borgani 2012) the processes governing the thermodynamical state of the outer regions in clusters: clumping of the gas, departures from hydrostatic equilibrium, contribution from non-thermal pressure by the presence of magnetic fields and/or cosmic rays, etc.

In this short overview, I reviewed some of the recent results from SZ observations. The included references provide the needed readings to further comprehend and illustrate the huge advances in this field achieved in the last decade. Future instruments or upgrade of existing instruments dedicated to the measurement of the SZ effect will increase spatial resolution and sensitivity providing enhanced abilities to understand clusters of galaxies from the detail of their central parts out to large radii.

References

Andersson, K., et al. 2011, ApJ, 738, 48
Angulo, R. E., et al. 2012, MNRAS, 426, 2046
Arnaud, M., et al. 2010, A&A, 517, A92
Benson, B. A., et al. 2004, ApJ, 617, 829
Benson, B. A., et al. 2011, eprint ArXiv:1112.5435
Bleem, L. E., et al. 2012, Nature, 753, L9
Bonamente, M., et al. 2008, ApJ, 675, 106

Carlstrom, J. E., et al. 2011, PASP, 123, 568

Croston, J. H., et al. 2008, A&A, 487, 431

da Silva, A. C., Kay, S. T., Liddle, A. R., & Thomas, P. A. 2004, MNRAS, 348, 1401

Dicker, S. R., et al. 2008, SPIE Conference Series, 7020

Dobbs, M., et al. 2006, New Astron. Rev., 50, 960

Draper, P., Dodelson, S., Hao, J., & Rozo, E. 2012, Phys. Rev. D, 85, 023005

Dunkley, J., et al. 2011, ApJ, 739, 52

Hasselfield, M., et al. 2013, Nature

Ho, P. T. P., et al. 2004, Modern Physics Letters A, 19, 993

Keisler, R., et al. 2011, ApJ, 743, 28

Komatsu, E., et al. 2001, PASJ, 53, 57

Kompaneets, A. S. 1957, Soviet Phys. — JETP Lett., 4, 730

Kosowsky, A. 2003, New Astron. Rev., 47, 939

Kravtsov, A. V. & Borgani, S. 2012, ARA&A, 50, 353

Liao, Y.-W., et al. 2010, ApJ, 713, 584

Marrone, D. P., et al. 2012, ApJ, 754, 119

Melin, J.-B., et al. 2011, A&A, 525, A139

Menanteau, F., et al. 2012, ApJ, 748, 7

Meneghetti, M., et al. 2010, A&A, 514, A93

Mroczkowski, T., et al. 2012, ApJ, 761, 47

Muchovej, S., et al. 2007, ApJ, 663, 708

Nagai, D., Kravtsov, A. V., & Vikhlinin, A. 2007, ApJ, 668, 1

Okabe, N., et al. 2010, ApJ, 721, 875

Pacaud, F., et al. 2007, MNRAS, 382, 1289

Planck Collaboration I. 2011, A&A, 536, A1

Planck Collaboration III. 2012, Submitted to A&A

Planck Collaboration IV. 2012, Submitted to A&A

Planck Collaboration IX. 2011, A&A, 536, A9

Planck Collaboration V. 2012, Submitted to A&A

Planck Collaboration VIII. 2011, A&A, 536, A8

Planck Collaboration X. 2011, A&A, 536, A10

Planck Collaboration XI. 2011, A&A, 536, A11

Planck Collaboration XXVI. 2011, A&A, 536, A26

Pointecouteau, E., Giard, M., & Barret, D. 1998, A&A, 336, 44

Pointecouteau, E., et al. 2001, ApJ, 552, 42

Pratt, G. W., Croston, J. H., Arnaud, M., & Böhringer, H. 2009, A&A, 498, 361

Reichardt, C. L., et al. 2013, ApJ, 763, 127

Sayers, J., et al. 2013, ApJ, 768, 177

Sazonov, S. Y. & Sunyaev, R. A. 1998, ApJ, 508, 1

Sehgal, N., et al. 2013, ApJ, 767, 38

Semler, D. R., et al. 2012, ApJ, 761, 183

Sievers, J. L., et al. 2013, Nature

Sifon, C., et al. 2013, ApJ, 772, 25

Simionescu, A., et al. 2011, Science, 331, 1576

Song, J., et al. 2012, Nature

Staniszewski, Z., et al. 2009, ApJ, 701, 32

Sun, M. 2012, New Journal of Physics, 14, 045004

Sunyaev, R. A. & Zeldovich, Y. B. 1972, Comments on Astrophysics and Space Physics, 4, 173

Vikhlinin, A., et al. 2006, ApJ, 640, 691

Voit, G. M. 2005, Reviews of Modern Physics, 77, 207

Zwart, J. T. L., et al. 2008, MNRAS, 391, 1545